Polymer Chemistry

PAPER

View Article Online
View Journal | View Issue

Cite this: *Polym. Chem.*, 2016, **7**, 1987

Tandem vinyl insertion-/ring-opening metathesis copolymerization with *ansa*-6-[2-(dimesitylboryl)-phenyl]pyrid-2-ylamido zirconium complexes: role of trialkylaluminum and MAO†

Min Wang,[a] Dongren Wang,[a] Laura Widmann,[a] Wolfgang Frey[b] and Michael R. Buchmeiser*[a,c]

Received 15th January 2016,
Accepted 14th February 2016

DOI: 10.1039/c6py00078a

www.rsc.org/polymers

The novel dialkylzirconium complexes **L′ZrR$_2$**, (R = CH_3, Bn = benzyl, CH_2SiMe_3, L′ = $Me_2Si\{\eta^5$-tetramethylcyclopentadienyl$\}$\{6-[2-(dimesitylboryl)phenyl]pyrid-2-ylamido\}) were synthesized. Upon activation with 1 equiv. of $[Ph_3C]^+[B(C_6F_5)_4]^-$, both **L′Zr(CH$_3$)$_2$** and **L′Zr(Bn)$_2$** are quantitatively converted *in situ* into **[L′Zr(CH$_3$)]$^+$[B(C$_6$F$_5$)$_4$]$^-$** and **[L′Zr(Bn)]$^+$[B(C$_6$F$_5$)$_4$]$^-$** while only 28 mol% conversion is observed with **L′Zr(CH$_2$SiMe$_3$)$_2$**. The aluminum-free cationic catalysts **[L′Zr(CH$_3$)]$^+$[B(C$_6$F$_5$)$_4$]$^-$**, **[L′Zr(Bn)]$^+$[B(C$_6$F$_5$)$_4$]$^-$** and **[L′Zr(CH$_2$SiMe$_3$)]$^+$[B(C$_6$F$_5$)$_4$]$^-$** initiate ring-opening metathesis polymerization (ROMP) of NBE to form predominantly *cis*-poly(NBE)$_{ROMP}$. Upon activation with $[Ph_3C]^+[B(C_6F_5)_4]^-$ and Al^iBu_3, **L′Zr(CH$_3$)$_2$**, **L′Zr(Bn)$_2$** and **L′Zr(CH$_2$SiMe$_3$)$_2$** also exhibit moderate catalytic activity in the copolymerization of ethylene (E) with NBE. The resulting copolymers do not contain any ROMP-derived poly(NBE), which is in stark contrast to the complexes' homopolymerization propensity for NBE. Upon activation with methylalumoxane (MAO), **L′Zr(CH$_3$)$_2$** and **L′Zr(Bn)$_2$** produce pure vinyl-insertion polymerization-derived poly(NBE)-*co*-poly(E) while **L′Zr(CH$_2$SiMe$_3$)$_2$** allows for the synthesis of predominantly *trans*-poly(NBE)$_{ROMP}$-*co*-poly(NBE)$_{VIP}$-*co*-poly(E)-based copolymers *via* an α-H$^+$ elimination/addition process. Our findings are discussed on the basis of the instability of the alkylidenes in the presence of E and the blocking effect of aluminum alkyls on ROMP *via* coordination to the pyridyl-moiety in the cationic complexes.

Introduction

Group 4 transition-metal monocyclopentadienyl-amido complexes are of considerable interest due to their remarkable activity in α-olefin polymerization.[1–3] The ability to additionally incorporate bulkier olefins, *e.g.*, norborn-2-ene (NBE), has attracted significant attention.[4] Introduction of alkyl substituents instead of halides has a significant impact on the reactivity of group 4 initiators and affects both catalytic activity and polymer properties such as molecular weight and comonomer incorporation.[5,6] Generally, metal alkyl cations, formed from the neutral dialkyl progenitor complexes upon activation with co-catalysts, *e.g.*, $[HNMe_2Ph]^+[B(C_6F_5)_4]^-$, $B(C_6F_5)_3$ or trityl borate $[Ph_3C]^+[B(C_6F_5)_4]^-$,[7] are assumed to represent the active species in olefin polymerization.

Our previous studies[8] revealed that group 4 metal dichloro complexes of the general formula **L′MCl$_2$** (M = Ti, Zr; L′ = $Me_2Si\{\eta^5$-tetramethylcyclopentadienyl$\}$\{6-[2-(R′$_2$-boryl)phenyl]pyrid-2-ylamido\}, R′ = *e.g.*, mesityl, ethyl, Scheme 1) activated by methylalumoxane (MAO) allow the synthesis of ethylene-norborn-2-ene (E-NBE) copolymers with both ring-opening metathesis polymerization (ROMP)- and vinyl-insertion polymerization (VIP)-derived poly(NBE) sequences within one single polymer chain, that is poly(NBE)$_{ROMP}$-*co*-poly(NBE)$_{VIP}$-*co*-poly(E) (Fig. 1). This was explained by a switch from VIP to ROMP *via* α-H$^+$ elimination from the growing polymer chain by the pyridyl nitrogen.

This switch can be tuned *via* the temperature-dependent dissociation of the N–B bond[9] for which detailed variable-temperature ^{1}H and ^{11}B NMR measurements have been carried out.

[a]*Lehrstuhl für Makromolekulare Stoffe und Faserchemie, Institut für Polymerchemie, Universität Stuttgart, Pfaffenwaldring 55, D-70569 Stuttgart, Germany. E-mail: michael.buchmeiser@ipoc.uni-stuttgart.de; Fax: +49(0)-711-685-64050*
[b]*Institut für Organische Chemie, Universität Stuttgart, Pfaffenwaldring 55, D-70569 Stuttgart, Germany*
[c]*Institut für Textilchemie und Chemiefasern (ITCF) Denkendorf, Körschtalstr. 26, D-73770 Denkendorf, Germany*

†Electronic supplementary information (ESI) available: ^{1}H-, ^{13}C-NMR spectra and crystallographic data for **L′Zr(CH$_3$)$_2$**, **L′Zr(Bn)$_2$** and **L′Zr(CH$_2$SiMe$_3$)$_2$**, ^{1}H-, ^{13}C-, ^{19}F-NMR spectra of **[L′Zr(CH$_3$)]$^+$[B(C$_6$F$_5$)$_4$]$^-$**, **[L′Zr(Bn)]$^+$[B(C$_6$F$_5$)$_4$]$^-$** and ^{1}H-NMR spectra of **[L′Zr(CH$_2$SiMe$_3$)]$^+$[B(C$_6$F$_5$)$_4$]$^-$** and of homo- and copolymers. CCDC 1440878 (**L′Zr(CH$_3$)$_2$**), 1440879 (**L′Zr(Bn)$_2$**) and 1440880 (**L′Zr(CH$_2$SiMe$_3$)$_2$**). For ESI and crystallographic data in CIF or other electronic format see DOI: 10.1039/c6py00078a

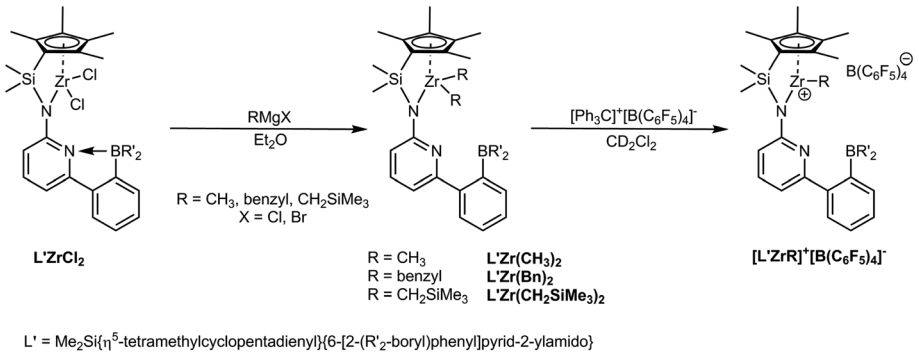

Scheme 1 Synthesis of $L'Zr(CH_3)_2$, $L'Zr(Bn)_2$, $L'Zr(CH_2SiMe_3)_2$ and the corresponding cationic complexes. Here, R′ = mesityl.

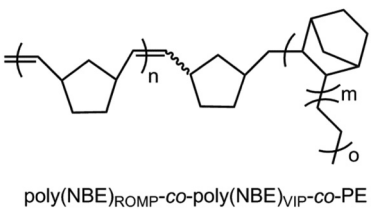

Fig. 1 Proposed structure of ROMP/VIP-derived poly(NBE)-*co*-poly(E) produced by $L'MCl_2$/MAO.[9]

With the aid of a variety of different pre-catalysts, the following key features have already been identified:[8–14] (i) a crowded ligand sphere around the metal favors the α-H^+ elimination process, *i.e.* the switch from VIP to ROMP, (ii) high NBE concentrations are required to support this switch from VIP to ROMP, and (iii) the propensity of the pyridine group to coordinate to boron can be governed by the sterics of the substituents at boron.

Unfortunately, the catalytic system $L'ZrCl_2$/MAO displays a low activity in E-NBE copolymerization (≤6 kg of polymer $mol^{-1}{}_{catalyst}\ h^{-1}\ bar^{-1}$), which has been attributed to the bulky ligand sphere and the propensity of the alkylidene to undergo cross metathesis with ethylene.[12] Generally, cationic M-alkyl catalysts derived from $L'MR_2$ *via* borane- or borate-activation have been demonstrated to display higher polymerization activity than the corresponding cationic M-alkyl catalysts derived from $L'MCl_2$/MAO. This can be explained by the fact that catalysts of the type $[L'MR]^+[BAr^F]^-$ are truly catalytic species while the systems $L'MR^+$/MAO in fact exist in the form of ion pairs or even adducts of the general formula $[L'M(\mu\text{-}R)_2AlR_2]^+[RMAO]^-$.[7,15–17]

Here, we report on structural modifications on the half-sandwich zirconium dichlorides ($L'ZrCl_2$) by replacement of both chloro ligands by dialkyl groups (alkyl = CH_3, benzyl, CH_2SiMe_3). The desired cationic complexes were then prepared *via* treatment of the dialkyl complexes with a stoichiometric amount of $[Ph_3C]^+[B(C_6F_5)_4]^-$. The catalytic performance of the cationic complexes in the homopolymerization of both NBE and E as well as in the copolymerization of E with NBE was explored in comparison to the parent dichloro-complex $L'ZrCl_2$, activated by MAO.

Results and discussion

$L'ZrCl_2$ was prepared as reported.[12] Treatment of $L'ZrCl_2$ with the corresponding Grignard reagents in diethyl ether[18–24] resulted in the formation of the dialkylzirconium complexes $L'Zr(CH_3)_2$, $L'Zr(Bn)_2$ (Bn = benzyl) and $L'Zr(CH_2SiMe_3)_2$. The synthetic routes are outlined in Scheme 1. Crystals suitable for single-crystal X-ray diffraction were grown from saturated diethyl ether solution. $L'Zr(CH_3)_2$ crystalizes in the triclinic space group $P\bar{1}$, a = 868.85(10), b = 1218.49(12), c = 1810.5(2) pm, α = 79.834°, β = 85.356°, γ = 81.823°, Z = 2 (Fig. 2). The $Zr(1)\text{–}N_{amide}$ distance is 216.0(2) pm, which is longer than in $L'ZrCl_2$ (210.85 pm). The pyridyl nitrogen is coordinated to zirconium (Zr(1)–N(2) = 253.9 pm) and not to the boron atom. Both the $Zr\text{–}N_{pyridine}$ and the $Zr\text{–}N_{amide}$ distances are longer than in $L'ZrCl_2$ (Table 1), which is attributed to the electron-donating property of the dimethyl groups.

$L'Zr(Bn)_2$ crystalizes in the monoclinic space group $P2_1/c$, a = 2791.4(2), b = 1601.47(9), c = 1021.51(7) pm, α = 90°, β = 95.322°, γ = 90°, Z = 4 (Fig. 3). The pyridyl nitrogen in $L'Zr(Bn)_2$ is neither coordinated to zirconium nor to the boron atom, which is in stark contrast to the situation in $L'ZrCl_2$ and $L'Zr(CH_3)_2$. We tentatively attribute this finding to the increased steric demand of the benzyl groups. The $Zr(1)\text{–}N_{amide}$ distance is 208.9(6) pm, which is significantly shorter than in $L'Zr(CH_3)_2$ (216.0 pm), attributable to the fact that the pyridine is uncoordinated. The angles C(42)–C(41)–Zr(1) and C(49)–C(48)–Zr(1) are 123.6(3)° and 91.1(3)°, respectively, which reveals that two benzyl ligands are inequivalent in the solid state, one adopting an η^1-bonding mode (123.6°) and the other η^2-bonding[25–30] (91.1°). In contrast to the solid state, the two benzyl groups in $L'Zr(Bn)_2$ are magnetically equivalent in solution (CD_2Cl_2), with two diastereotopic benzylic protons at δ = 2.06 and 1.93 ppm (J = 52.0 Hz).

$L'Zr(CH_2SiMe_3)_2$ (Fig. 4) crystalizes in the triclinic space group $P\bar{1}$, a = 1114.92(5), b = 1131.88(5), c = 2027.72(9) pm, α = 89.308°, β = 82.967°, γ = 77.549°, Z = 2. The pyridyl nitrogen is neither coordinated to Zr nor to B, similar to $L'Zr(Bn)_2$. The $Zr(1)\text{–}N_{amide}$ distance is 213.23(11) pm, which is shorter than in $L'Zr(CH_3)_2$ (216.0 pm) but longer than in $L'Zr(Bn)_2$ (208.9 pm).

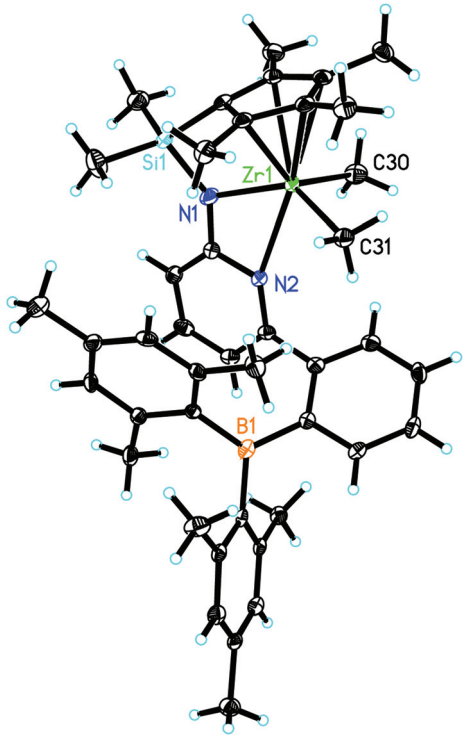

Fig. 2 Single-crystal X-ray structure of **L′Zr(CH$_3$)$_2$**. Selected bond lengths [pm] and angles [°]: Zr(1)–N(1) 216.0(2), Zr(1)–C(30) 224.4(2), Zr(1)–C(31) 226.9(3), Zr(1)–C(34) 247.3(2), Zr(1)–C(35) 248.4(3), Zr(1)–C(38) 251.4(2), Zr(1)–N(2) 253.9(2), Zr(1)–C(36) 258.1(3), Zr(1)–C(37) 258.1(2), Zr(1)–C(1) 283.7(3); N(1)–Zr(1)–C(30) 107.52(10), N(1)–Zr(1)–C(31) 132.95(9), C(30)–Zr(1)–C(31) 102.70(10), N(1)–Zr(1)–N(2) 56.29(7), C(30)–Zr(1)–N(2) 90.31(8), C(31)–Zr(1)–N(2) 88.90(8).

Table 1 Selected bond lengths [pm] for **L′ZrCl$_2$**, **L′Zr(CH$_3$)$_2$**, **L′Zr(Bn)$_2$** and **L′Zr(CH$_2$SiMe$_3$)$_2$**

#	**L′ZrCl$_2$**	**L′Zr(CH$_3$)$_2$**	**L′Zr(Bn)$_2$**	**L′Zr(CH$_2$SiMe$_3$)$_2$**
Zr–N$_{amide}$	210.85	216.0	208.9	213.23
Zr–N$_{pyridine}$	249.61	253.9	—	—
Zr–C$_{alkyl}$	—	224.4/226.9	226.2/227.9	224.3/225.5

The corresponding cationic complexes were created *in situ* by abstraction of one alkyl group from the corresponding dialkyl complexes using 1 equiv. of [Ph$_3$C]$^+$[B(C$_6$F$_5$)$_4$]$^-$ in CD_2Cl_2 [31,32] (Scheme 1). For **L′Zr(CH$_3$)$_2$** and **L′Zr(Bn)$_2$**, ^{1}H NMR spectroscopy was indicative for the quantitative conversion of the dialkyl complexes to the corresponding cationic complexes. However, addition of [Ph$_3$C]$^+$[B(C$_6$F$_5$)$_4$]$^-$ to a CD_2Cl_2 solution of **L′Zr(CH$_2$SiMe$_3$)$_2$** resulted only in ~28 mol% formation of the cationic complex, probably due to the sterics of two CH_2SiMe_3 groups at the metal and their low reactivity with [Ph$_3$C]$^+$[B(C$_6$F$_5$)$_4$]$^-$. Among these monoalkyl cationic complexes, isolation of the methyl cation with one diethyl ether molecule coordinated to Zr as indicated by NMR and elemental analysis was successful.

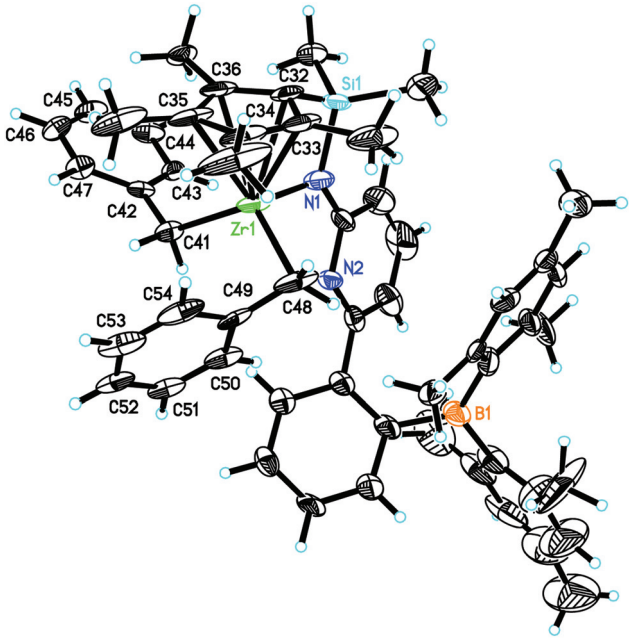

Fig. 3 Single-crystal X-ray structure of **L′Zr(Bn)$_2$**. Selected bond lengths [pm] and angles [°]: Zr(1)–N(1) 208.9(6), Zr(1)–C(48) 226.2(5), Zr(1)–C(41) 227.9(5), Zr(1)–C(32) 243.3(5), Zr(1)–C(33) 247.4(5), Zr(1)–C(34) 260.0(6), Zr(1)–C(35) 257.7(7), Zr(1)–C(36) 251.4(5); N(1)–Zr(1)–C(48) 109.8(2), N(1)–Zr(1)–C(41) 102.59(19), C(48)–Zr(1)–C(41) 117.38(19), C(42)–C(41)–Zr(1) 123.6(3), C(49)–C(48)–Zr(1) 91.1(3).

Dialkyl complexes are also valuable progenitors for the formation of metal alkylidenes through thermally induced α-H elimination.[33] Alternatively, α-hydrogen abstraction can be induced by the addition of phosphines (PMe$_3$, PPhMe$_2$, PPh$_2$Me, *etc.*).[34–39] The resulting alkylidenes are the key species in metathesis polymerization. Unfortunately, all attempts to generate metal alkylidenes through thermolysis or by the addition of phosphines to the neutral alkyl compounds were unsuccessful. Thus, in toluene-d$_8$, **L′Zr(CH$_3$)$_2$**, **L′Zr(Bn)$_2$**, **L′Zr(CH$_2$SiMe$_3$)$_2$** were found to be thermally stable at least up to 80 °C. The same accounts for **[L′Zr(CH$_3$)]$^+$**, **[L′Zr(Bn)]$^+$** and **[L′Zr(CH$_2$SiMe$_3$)]$^+$[B(C$_6$F$_5$)$_4$]$^-$** in *o*-C$_6$D$_4$Cl$_2$. Even in the presence of 3–7 equiv. of PMe$_3$ or PPhMe$_2$ with respect to Zr, no transformation of the Zr-dialkyls to the corresponding Zr-alkylidenes was observed by ^{1}H NMR.

NBE homopolymerization and E-NBE copolymerization

Ring-opening metathesis homopolymerization of NBE by the action of *in situ* generated **[L′Zr(CH$_3$)]$^+$**, **[L′Zr(Bn)]$^+$** and **[L′Zr(CH$_2$SiMe$_3$)]$^+$[B(C$_6$F$_5$)$_4$]$^-$** was carried out in toluene at different temperatures (Table 2). Notably, productivity of **[L′Zr(Bn)]$^+$[B(C$_6$F$_5$)$_4$]$^-$** at 80 °C was remarkably higher (140 kg of polymer mol$^{-1}_{catalyst}$ h^{-1}) than that of **[L′Zr(CH$_3$)]$^+$** and **[L′Zr(CH$_2$SiMe$_3$)]$^+$[B(C$_6$F$_5$)$_4$]$^-$**, which is attributable to a higher propensity of **[L′Zr(Bn)]$^+$** to form **L′Zr=CHPh**. Interestingly, all polymers were purely ROMP-derived poly(NBE) and did not contain any VIP-type poly(NBE) as evidenced by ^{13}C NMR (Fig. S1b–S4b, ESI†). The *cis*-content of the polymers increased

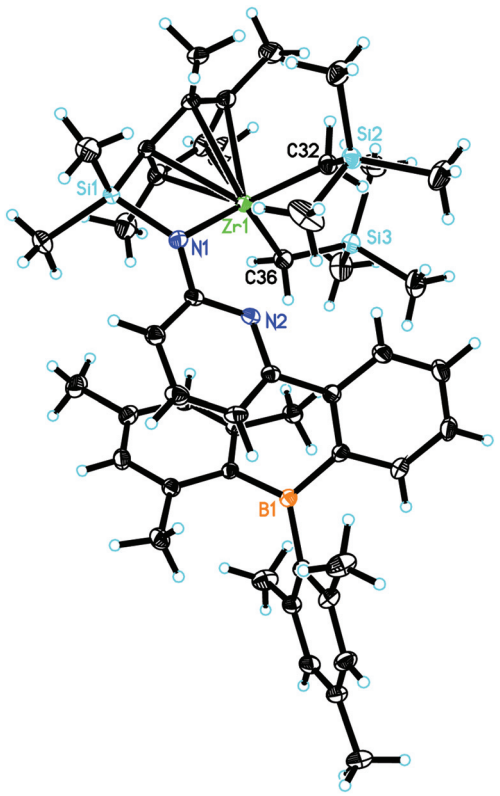

Fig. 4 Single-crystal X-ray structure of **L′Zr(CH$_2$SiMe$_3$)$_2$**. Selected bond lengths [pm] and angles [°]: Zr(1)–N(1) 213.23(11), Zr(1)–C(32) 224.30(13), Zr(1)–C(36) 225.50(14), Zr(1)–C(40) 246.68(13), Zr(1)–C(44) 248.05(13), Zr(1)–C(41) 252.47(13), Zr(1)–C(43) 259.96(13), Zr(1)–C(42) 261.18(13); N(1)–Zr(1)–C(32) 111.58(5), N(1)–Zr(1)–C(36) 103.35(5), C(32)–Zr(1)–C(36) 103.35(5), Si(2)–C(32)–Zr(1) 130.85(7), Si(3)–C(36)–Zr(1) 126.57(7).

Table 2 Results for NBE homopolymerization (ROMP) by the action of **L′Zr(CH$_3$)$_2$**, **L′Zr(Bn)$_2$** and **L′Zr(CH$_2$SiMe$_3$)$_2$** activated by [Ph$_3$C]$^+$[B(C$_6$F$_5$)$_4$]$^-$ [a]

#	Catalyst	T (°C)	A [b]	M_n [c] (g mol^{-1})	$Đ$ [c]	T_g [d] (°C)	*cis* [e] (%)
1	**L′Zr(CH$_3$)$_2$**	50	10	170 000	2.7	58	85
2	**L′Zr(CH$_3$)$_2$**	65	12	92 000	2.5	56	71
3	**L′Zr(CH$_3$)$_2$**	80	45	10 000	1.6	47	52
4	**L′Zr(Bn)$_2$**	50	2	—	—	48	69
5	**L′Zr(Bn)$_2$**	65	10	100 000	3.1	53	70
6	**L′Zr(Bn)$_2$**	80	140	14 000	2.2	39	72
7	**L′Zr(CH$_2$SiMe$_3$)$_2$**	50	5	200 000	2.1	45	72
8	**L′Zr(CH$_2$SiMe$_3$)$_2$**	65	10	43 000	1.1	50	71
9	**L′Zr(CH$_2$SiMe$_3$)$_2$**	80	9	21 000	1.9	53	61

[a] 100 mL Schlenk flask, total volume of reaction mixture: 50 mL of toluene, [catalyst] = 1 × 10^{-4} mol L^{-1}, catalyst : [Ph$_3$C]$^+$[B(C$_6$F$_5$)$_4$]$^-$: NBE = 1 : 1 : 10 000, t = 1 h. [b] Activity in kg of polymer mol$^{-1}_{catalyst}$ h^{-1}. [c] Molecular weights (M_n) and polydispersity indexes ($Đ$) determined by HT-GPC in 1,2,4-trichlorobenzene *vs.* PS. [d] Measured by DSC. [e] Determined by ^{1}H NMR analysis in 1,1,2,2-tetrachloroentane-d$_2$.

with decreasing polymerization temperature (52 < σ_{cis} < 85%, Fig. S1a–S4a, ESI†) and correlated with T_g;[40] however, it was lower (Fig. S1a–S4a, ESI†) than that in poly(NBE)s prepared by the action of **L′ZrCl$_2$**/MAO (86 < σ_{cis} < 95%).[12] This points towards stronger ion pairing of the cations with MAO than with the [B(C$_6$F$_5$)$_4$]$^-$ anion and consequently a significant influence of the large MAO on the geometry of the active centers. In terms of mechanism, the formation of poly(NBE)$_{ROMP}$ must proceed by the formation of zirconium alkylidenes,[34–39,41–48] promoted by the approach of NBE molecules or by the NBE insertion into the metal–carbon bond of the parent cationic system followed by α-hydrogen abstraction (Scheme 2, *vide infra*). However, no alkylidene species were spectroscopically detectable. Obviously, only minor amounts of the corresponding cations convert into alkylidenes. The comparably high polydispersity indexes are tentatively attributed to secondary metathesis, *i.e.* to back-biting.

Cationic group 4 transition-metal alkyl complexes have been reported to exhibit high catalytic activity and efficient incorporation of bulky comonomers in the absence of aluminum co-catalysts.[5,6,49,50] It was therefore of interest to explore the copolymerization of E with NBE with **[L′Zr(CH$_3$)]$^+$**, **[L′Zr(Bn)]$^+$** and **[L′Zr(CH$_2$SiMe$_3$)]$^+$[B(C$_6$F$_5$)$_4$]$^-$**. Unfortunately, none of these catalysts was capable of homopolymerizing E or copolymerizing E with NBE to yield high molecular weight (co-)polymers without the involvement of aluminum alkyl activators. For reasons, *vide infra*.

Upon *in situ* activation with [Ph$_3$C]$^+$[B(C$_6$F$_5$)$_4$]$^-$ and triisobutylaluminum (Al^{i}Bu$_3$),[51–60] **L′Zr(CH$_3$)$_2$**, **L′Zr(Bn)$_2$** and **L′Zr(CH$_2$SiMe$_3$)$_2$** showed moderate catalytic activity in E-NBE copolymerization ranging from 15 to 80 kg of polymer mol$^{-1}_{catalyst}$ h^{-1} bar^{-1}, which is significantly higher than the activity of **L′ZrCl$_2$**/MAO (≤4 kg of polymer mol$^{-1}_{catalyst}$ h^{-1} bar^{-1})[12] under similar conditions (Table 3, entries 2–6). It is worth noting that **L′Zr(Bn)$_2$** exhibited the highest productivity (80 kg of polymer mol$^{-1}_{catalyst}$ h^{-1} bar^{-1}) in E-NBE copolymerization, in line with its highest activity in NBE homopolymerization (*vide supra*). This high activity of **[L′Zr(Bn)]$^+$[B(C$_6$F$_5$)$_4$]$^-$** might be attributed to a reversible η^2–η^1 rearrangement of the benzylic group, which stabilizes the active sites and reduces deactivation.[15] Generally, NBE incorporation into the copolymers was low (≤2 mol%) compared to the one obtained with **L′ZrCl$_2$**/MAO (28 mol%) under similar conditions.[12] Solely VIP-derived poly(NBE) moieties were observed in poly(E)-*co*-poly(NBE) (Fig. 5). The characteristic resonances at δ = 47.0 (C$_2$/C$_3$), 41.5 (C$_1$/C$_4$) and 32.9 (C$_7$) ppm are assignable to alternating syndiotactic (*alt-st*, E-NBE-E-NBE)/isolated (E-NBE-E-E) VIP-derived sequences while the signal at δ = 29.5 ppm corresponds to PE sequences.[61,62] Also, no signals for alternating isotactic (*alt-it*, E-NBE-E-NBE) units, NBE diads (E-NBE-NBE-E) or triads (E-NBE-NBE-NBE-E) were observed. Although the *alt-st* and isolated NBE sequences cannot be distinguished as a result of overlapping signals, it is with respect to the low NBE incorporation and the bulky ligand sphere reasonable to propose isolated NBE sequences. ^{13}C NMR analysis proved that PE sequences in the copolymers were mostly mainly linear with low degrees of branching (~1 branch per 1000 carbons), indicative for a low β-hydride elimination and chain-walking propensity.

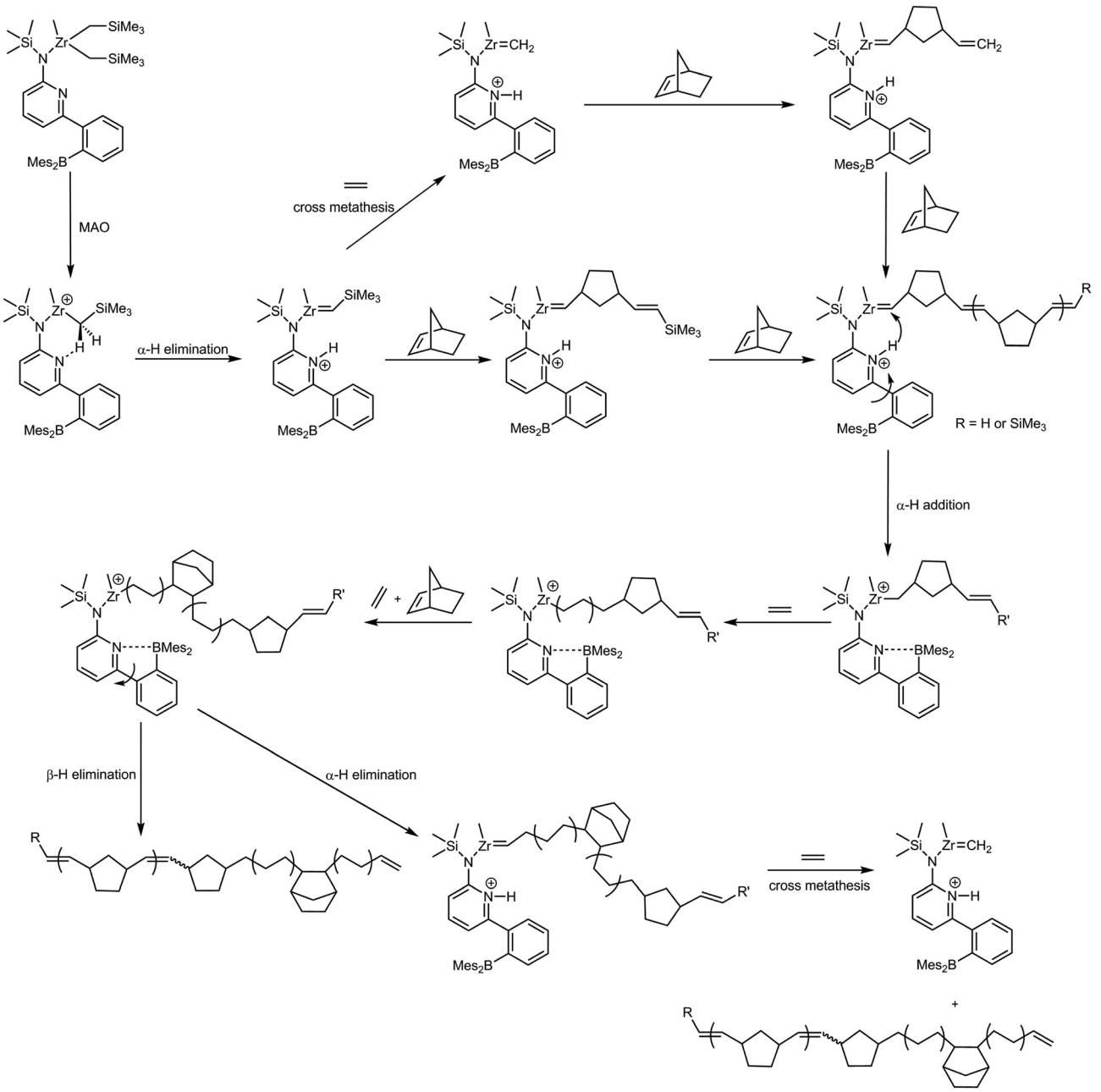

Scheme 2 Proposed mechanism for the formation of poly(NBE)$_{ROMP}$-*co*-poly(NBE)$_{VIP}$-*co*-poly(E) by the action of **L′Zr(CH$_2$SiMe$_3$)$_2$**/MAO.

In addition, a terminal vinyl group was observed in all PE sequences of copolymers as clearly demonstrated by multiplets at δ = 5.9 and 5.0 ppm in the ^{1}H NMR spectrum (Fig. S5, ESI†) and at δ = 139.3 and 114.1 ppm in the ^{13}C NMR spectrum[14] (Fig. 5). Similarly, the PE prepared from **L′Zr(CH$_3$)$_2$**/[Ph$_3$C]$^+$[B(C$_6$F$_5$)$_4$]$^-$/Al^{i}Bu$_3$ showed vinyl terminals (Fig. S6, ESI†); the PE itself was mainly linear with 2 branches per 1000 carbons as estimated by ^{13}C NMR (Fig. S7, ESI†). In combination with the melting point (T_m) of poly(E)-*co*-poly(NBE), which ranged from 129 to 131 °C and a single peak in the GPC, the structure of the copolymers produced by **L′Zr(CH$_3$)$_2$**, **L′Zr(Bn)$_2$** and **L′Zr(CH$_2$SiMe$_3$)$_2$** activated with [Ph$_3$C]$^+$-[B(C$_6$F$_5$)$_4$]$^-$ and Al^{i}Bu$_3$ was VIP-type poly(E)-*co*-poly(NBE) with few branches (Fig. 5 and Fig. S8–S9, ESI†). With **L′Zr(CH$_3$)$^+$**/Al^{i}Bu$_3$, an increase in polymerization temperature from 30 to 80 °C resulted in a dramatic decrease in molecular weight (M_n) from 570 000 to 32 000 g mol^{-1} and a significant increase in the polydispersity index ($Đ$) from 2.6 to 7.6, indicative for substantial β-hydride elimination/chain transfer to monomer.

Generally, AlR$_3$ plays an essential role in the polymerization process. In VIP, heterobimetallic complexes termed as [L′M(μ-R)$_2$AlR$_2$]$^+$ are considered to be the dormant species.[15,63–65] Consequently, subsequent dissociation of AlR$_3$ to form metal alkyl cations is the key step in olefin polymeri-

Table 3 Results for E homopolymerization by the action of **L′Zr(CH$_3$)$_2$** [a] and E-NBE copolymerization by the action of **L′Zr(CH$_3$)$_2$**, **L′Zr(Bn)$_2$** and **L′Zr(CH$_2$SiMe$_3$)$_2$** activated by [Ph$_3$C]$^+$[B(C$_6$F$_5$)$_4$]$^-$/Al^{i}Bu$_3$ [a] and MAO[b]

#	Catalyst	Monomers	T (°C)	A[c]	C_{NBE}[d] (mol%)	M_n[e] (g mol^{-1})	$Đ$[e]	T_m[f] (°C)
1[a]	**L′Zr(CH$_3$)$_2$**	E	50	30	—	1 000 000	2.9	129
2[a]	**L′Zr(CH$_3$)$_2$**	E/NBE	30	15	1.7	570 000	2.6	131
3[a]	**L′Zr(CH$_3$)$_2$**	E/NBE	50	60	1.5	300 000	4.3	129
4[a]	**L′Zr(CH$_3$)$_2$**	E/NBE	80	42	1.7	32 000	7.6	129
5[a]	**L′Zr(Bn)$_2$**	E/NBE	50	80	0.5	340 000	6.3	131
6[a]	**L′Zr(CH$_2$SiMe$_3$)$_2$**	E/NBE	50	45	2.0	>6 000 000	—	130
7[b]	**L′Zr(CH$_3$)$_2$**	E/NBE	50	4	1.1	>6 000 000	—	125
8[b]	**L′Zr(Bn)$_2$**	E/NBE	50	4	2.0	640 000	2.7	128
9[b]	**L′Zr(CH$_2$SiMe$_3$)$_2$**	E/NBE	30	5	3	490 000	2.5	123
10[b]	**L′Zr(CH$_2$SiMe$_3$)$_2$**	E/NBE	50	7	25	220 000	2.4	121
11[b]	**L′Zr(CH$_2$SiMe$_3$)$_2$**	E/NBE	80	3	19	660 000	4.6	126

[a] 250 mL of toluene (including the volume of monomer), t = 1 h, [catalyst] = 2 × 10^{-5} mol L^{-1}, catalyst : [Ph$_3$C]$^+$[B(C$_6$F$_5$)$_4$]$^-$: Al^{i}Bu$_3$ = 1 : 1 : 350 or catalyst : [Ph$_3$C]$^+$[B(C$_6$F$_5$)$_4$]$^-$: Al^{i}Bu$_3$: NBE = 1 : 1 : 350 : 20 000, $p_{ethylene}$ = 4 bar. [b] Catalyst : MAO : NBE = 1 : 2000 : 20 000, $p_{ethylene}$ = 4 bar. [c] Activity in kg of polymer mol$^{-1}_{catalyst}$ h^{-1} bar^{-1}. [d] NBE content in the copolymer [mol%] as estimated by ^{13}C NMR spectroscopy. [e] Molecular weights (M_n) and polydispersity indexes ($Đ$) determined by HT-GPC in 1,2,4-trichlorobenzene *vs.* PS. [f] Measured by DSC.

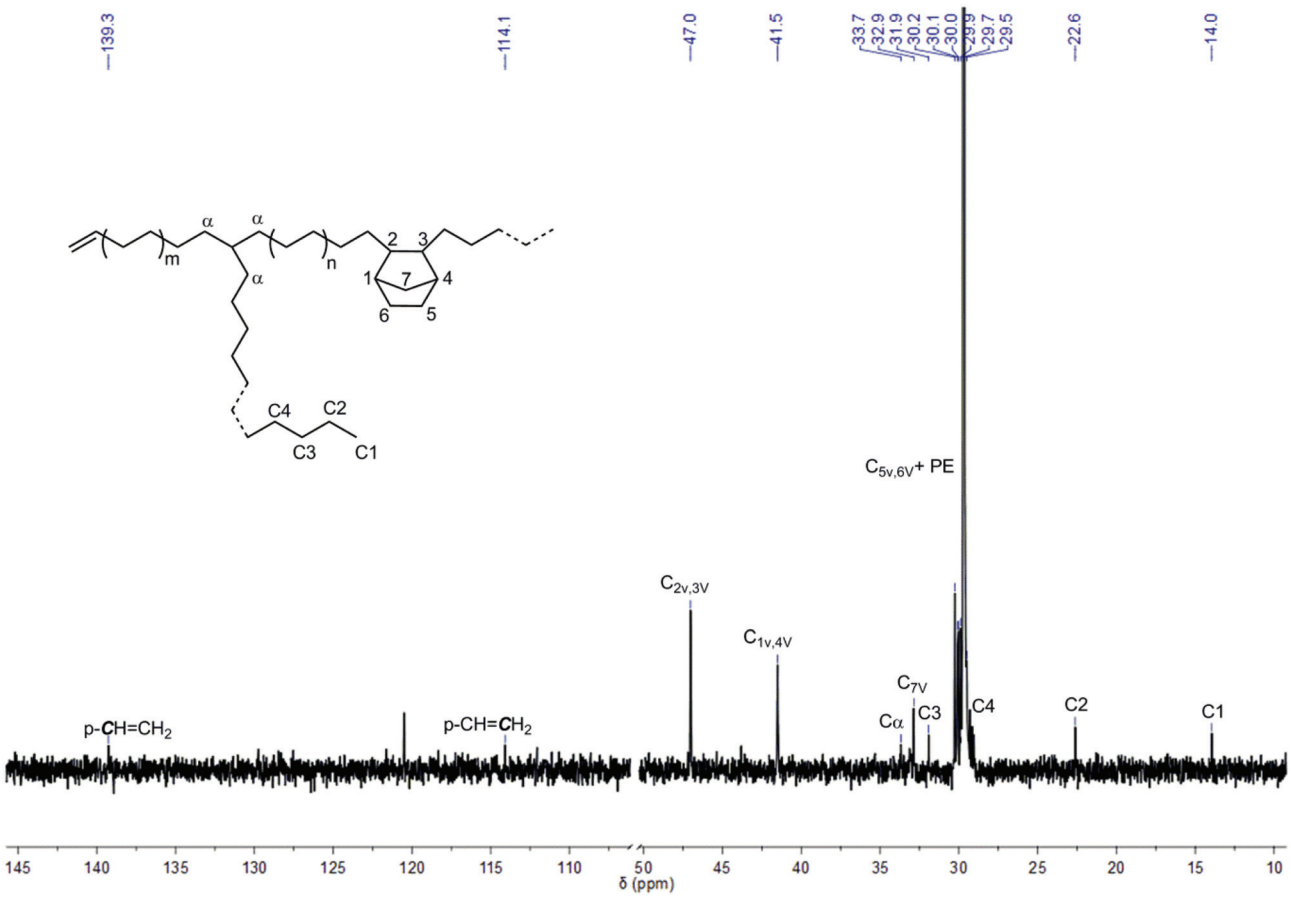

Fig. 5 ^{13}C NMR spectrum of poly(E)-*co*-poly(NBE)$_{VIP}$ produced by **L′Zr(CH$_3$)$_2$**/[Ph$_3$C]$^+$[B(C$_6$F$_5$)$_4$]$^-$/Al^{i}Bu$_3$ (Table 3, entry 4). The signal at δ = 120.5 ppm stems from the impurity in 1,1,2,2-tetrachloroethane-d$_2$.

zation.[15,66] The reversible coordination/decoordination of the pyridyl group in **L′ZrCl$_2$** has been shown to play a crucial role in the α-hydrogen abstraction process.[12] Unlike **L′ZrCl$_2$**, **L′Zr(CH$_3$)$_2$** displays only the "open" structure with no pyridyl coordination to boron as evidenced by ^{11}B NMR[67–69] (Fig. S10, ESI†), which is attributed to the electron richer nature of the complex. The boron signals in the ^{11}B NMR of **L′Zr(Bn)$_2$** and **L′Zr(CH$_2$SiMe$_3$)$_2$** are too weak and do not allow any conclusive structure assignment (*i.e.* coordinated *vs.* non-coordinated). However, in view of the similar electronic nature of the benzyl

and CH_2SiMe_3 groups and the solid state structures it is reasonable to assume that the pyridine group is not coordinated to boron in the temperature range of polymerization. The finding that $[\mathbf{L'ZrR}]^+[\mathbf{B(C_6F_5)_4}]^-$ (R = CH_3, Bn, CH_2SiMe_3) forms ROMP-derived poly(NBE) in the absence but not in the presence of Al^iBu_3 and that $[\mathbf{L'ZrR}]^+[\mathbf{B(C_6F_5)_4}]^-$ (R = CH_3, Bn, CH_2SiMe_3) does form VIP-derived poly(NBE)-*co*-poly(E) in the presence but not in the absence of Al^iBu_3 strongly suggests that Al^iBu_3 binds to the pyridyl-moiety in $[\mathbf{L'ZrR}]^+$, thereby terminating its capability to induce α-hydrogen abstraction, a process that occurs in the absence of Al^iBu_3. Accordingly, the cationic complexes are capable of forming VIP-derived poly(NBE)-*co*-poly(E) in the presence of Al^iBu_3, but not in its absence. In the absence of Al^iBu_3, α-H^+ elimination dominates and poly(NBE)$_{ROMP}$ forms. Notably, the isolated diethyl ether adduct $[\mathbf{L'Zr(CH_3)Et_2O}]^+[\mathbf{B(C_6F_5)_4}]^-$ is inactive in NBE homopolymerization in the absence of Al^iBu_3 and inactive in E-NBE copolymerization in the presence of Al^iBu_3, which clearly reveals the irreversible blocking effect of Et_2O on the coordination of olefin. It is also worth pointing out that any interaction between the metal and the $[B(C_6F_5)_4]^-$ anion, whether *via* the fluorines or *via* the phenyl-group itself, can be excluded to the greatest possible extent by the fact that the ^{19}F NMR spectra of $[\mathbf{L'ZrR}]^+[\mathbf{B(C_6F_5)_4}]^-$ (R = CH_3, Bn) do not show any differences to the one of $[Ph_3C]^+[B(C_6F_5)]^-$ (Fig. S11 and S33, S36, S39, ESI†). All in all, the inability of $\mathbf{L'ZrR}^+$ (R = CH_3, Bn, CH_2SiMe_3) to promote ROMP in the presence of Al^iBu_3 and to promote vinyl insertion copolymerization of E with NBE in the absence of Al^iBu_3 is attributed to the following three key features: (i) the instability of the alkylidenes in the presence of E, (ii) the blocking of the pyridyl ligand in $[\mathbf{L'ZrR}]^+$ by Al^iBu_3 and (iii) the competition of a coordinating solvent for the coordination site.

Next, the performance of $\mathbf{L'ZrR_2}$/MAO (R = CH_3, Bn, CH_2SiMe_3) in E-NBE copolymerization was explored in comparison to the one of $\mathbf{L'ZrCl_2}$/MAO and $[\mathbf{L'ZrR}]^+[B(C_6F_5)]^-$/$Al^iBu_3$ (R = CH_3, Bn, CH_2SiMe_3) (Table 3, entries 7–11). Catalytic activities were lower for the systems $\mathbf{L'ZrR_2}$/MAO (3–7 kg of polymer $mol^{-1}_{catalyst}$ h^{-1} bar^{-1}) and $\mathbf{L'ZrCl_2}$/MAO (1–4 kg of polymer $mol^{-1}_{catalyst}$ h^{-1} bar^{-1}) compared to $[\mathbf{L'ZrR}]^+[B(C_6F_5)]^-/Al^iBu_3$ (15–80 kg of polymer $mol^{-1}_{catalyst}$ h^{-1} bar^{-1}), which is in line with literature reports[7,15–17] (*vide supra*).

For the copolymers produced by $\mathbf{L'Zr(CH_3)_2}$/MAO and $\mathbf{L'Zr(Bn)_2}$/MAO, only VIP-derived poly(NBE)-*co*-poly(E) was obtained. Low NBE incorporation, *i.e.* 1.1 and 2.0 mol%, respectively, was observed along with vinyl terminals and few long chain branches (Fig. S12–S13, ESI†). By contrast, $\mathbf{L'Zr(CH_2SiMe_3)_2}$/MAO produced copolymers with both ROMP- and VIP-derived NBE units in the same polymer chain, that is poly(NBE)$_{ROMP}$-*co*-poly(NBE)$_{VIP}$-*co*-PE. At 30 °C, the ratio of poly(NBE)$_{ROMP}$: poly(NBE)$_{VIP}$: PE was 1 : 2 : 97 (Fig. S14–S15, ESI†) and increased to 22 : 3 : 75 with increasing temperature (50 °C) (Fig. 6a and Fig. S16–S18, ESI†). Again, terminal vinyl groups and few long chain branches were observed. A further increase in the temperature (80 °C) resulted in a decrease in the proportion of ROMP-type poly(NBE) units in the copolymers (14 : 5 : 81) (Fig. S19–S20, ESI†).

Signals at δ = 47.0 ($C_{2,3}$), 41.5 ($C_{1,4}$), 32.9 (C_7) and 30.2–29.9 ($C_{5,6}$) ppm can be attributed to *alt-st*/isolated VIP-derived poly(NBE) units; those at δ = 29.7 ppm are assignable to PE. As outlined above, isolated VIP-type NBE sequences interrupted by PE sequences are reasonable. This incapability to form consecutive VIP-derived NBE–NBE sequences also accounts for the finding that no VIP-derived sequences are visible in poly(NBE)$_{ROMP}$. The signals at δ = 134.2, 133.2 ($C_{2,3}$), 43.0, 38.8 ($C_{1,4}$), 42.8, 42.1, 41.4 (C_7) and 33.5, 32.5 ($C_{5,6}$) are unambiguously assignable to ROMP-derived NBE sequences. In contrast to poly(NBE)$_{ROMP}$-*co*-poly(NBE)$_{VIP}$-*co*-PE prepared by a structurally similar Ti-catalyst,[8] copolymers had a substantially higher *trans*-content with more tttt and cccc sequences (t = *trans*, c = *cis*). Notably, these signals prevail even after extensive hot extraction with THF. This together with the finding that poly(NBE)$_{ROMP}$ is a high *cis* polymer but poly(NBE)$_{ROMP}$-*co*-poly(NBE)$_{VIP}$-*co*-PE is predominantly *trans* and the unimodal GPC traces (Fig. S21†) strongly suggest that the ROMP-derived sequences are part of the entire polymer chain. Further evidence for the proposed copolymer structure (Fig. 6a) comes from the absence of any glass transition (Fig. S22†) attributable to pure poly(NBE)$_{ROMP}$. This absence of any poly(NBE)$_{ROMP}$-derived T_g in combination with the high incorporation of ROMP-derived poly(NBE) sequences (*vide supra*) also points towards a multi-block structure, however, without real proof.

Our plausible explanation for the formation of this unique polymer structure is an α-H^+ elimination/addition process as outlined in Scheme 2. According to our proposed scheme, $\mathbf{L'Zr(CH_2SiMe_3)_2}$ is activated by MAO to form the cationic species $\mathbf{L'Zr(CH_2SiMe_3)}^+$, which through α-$H^+$ elimination yields a Zr-alkylidene ($\mathbf{L'Zr{=}CHSiMe_3}$) that promotes ROMP of NBE. As outlined earlier,[8,12,13] substantial steric congestion is required to induce the switch from VIP to ROMP. In that regards, the CH_2SiMe_3 group acts similar, though less effective, than a NBE group between the metal and the polymer chain. In the presence of ethylene, $\mathbf{L'Zr{=}CHSiMe_3}$ yields a Zr-methylidene ($\mathbf{L'Zr{=}CH_2}$) *via* cross metathesis, which is also ROMP-active, too. The previous observation that with catalysts containing the 6-(2-BR'_2-phenyl)pyrid-2-ylamido motif (R′ = ethyl, mesityl) high NBE concentrations are needed to form any ROMP-derived sequences[8,10–13] strongly suggests that cross metathesis of any Zr-alkylidene with E to form Zr-methylidene is the predominant reaction in these systems. This is in line with the high diffusivity of E. The transient Zr-methylidene is presumably exhausted to most extent as a result of its low stability, *e.g. via* bimolecular decomposition,[12] which accounts for the low ROMP propensity and the low productivity of these pre-catalysts upon activation with MAO in E-NBE copolymerization. As already outlined, this accounts for the finding that no polymer is obtained in the copolymerization of E with NBE by the action of $[\mathbf{L'Zr(CH_3)}]^+$, $[\mathbf{L'Zr(Bn)}]^+$ or $[\mathbf{L'Zr(CH_2SiMe_3)}]^+[\mathbf{B(C_6F_5)_4}]^-$ in the absence of Al^iBu_3. In case polymerizations are activated with MAO, an α-hydrogen addition

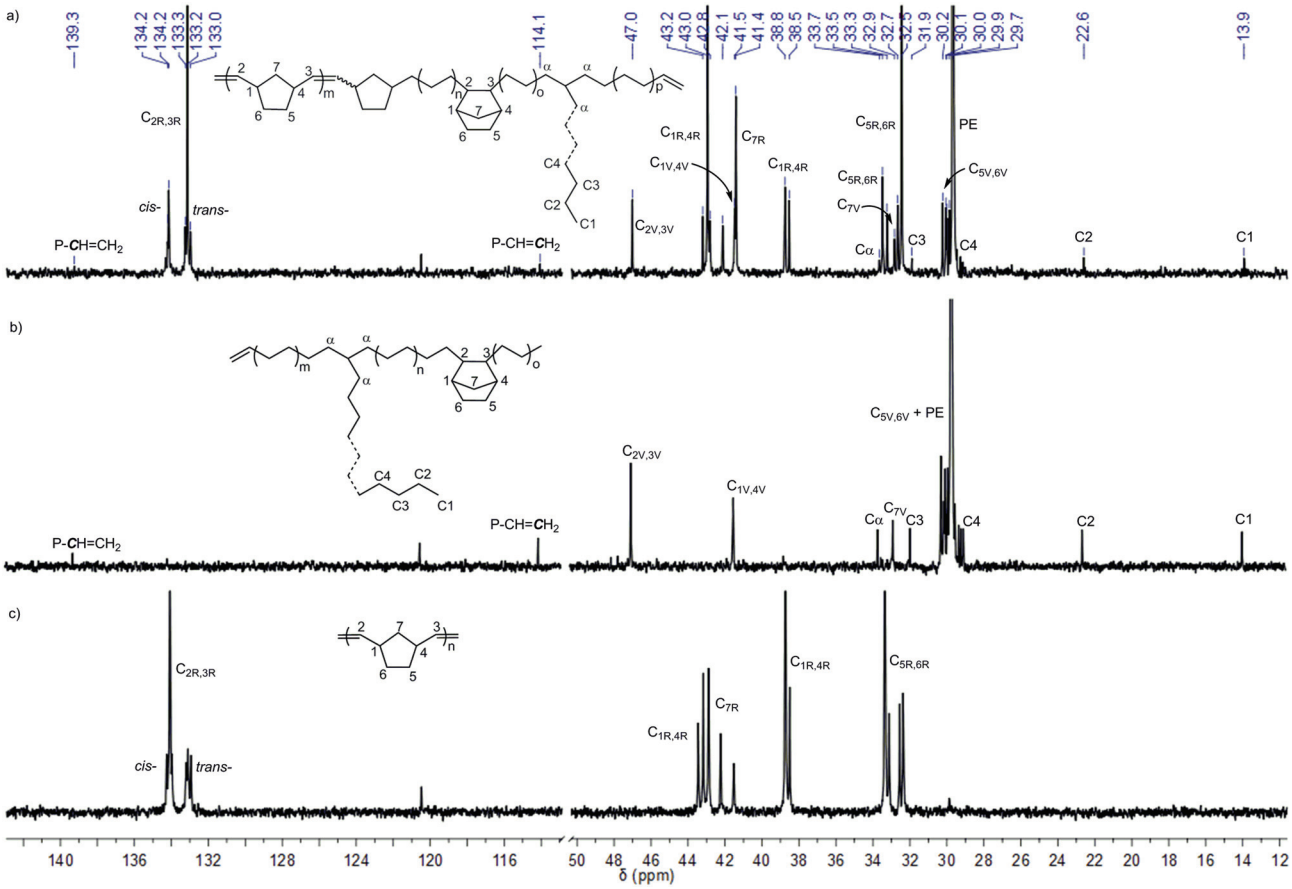

Fig. 6 ^{13}C NMR spectra of (a) poly(NBE)$_{ROMP}$-*co*-poly(NBE)$_{VIP}$-*co*-poly(E) produced by **L′Zr(CH$_2$SiMe$_3$)$_2$**/MAO (Table 3, entry 10), (b) poly(NBE)$_{VIP}$-*co*-poly(E) produced by **L′Zr(Bn)$_2$**/MAO (Table 3, entry 8) and (c) poly(NBE)$_{ROMP}$ produced by **L′Zr(CH$_2$SiMe$_3$)$_2$**/$[Ph_3C]^+[B(C_6F_5)_4]^-$ (Table 2, entry 8). The signal at δ = 120.5 ppm stems from the impurity in 1,1,2,2-tetrachloroethane-d_2.

to the ROMP-active species can re-establish the VIP-active species, which now incorporates E and NBE. During E-NBE insertion copolymerization, E incorporation is favored as evidenced by the high E content in the resulting E-NBE copolymers.

The proposed switch from ROMP to VIP, *i.e.* α-H$^+$ addition, is remarkable, since for such a step the pyridinium (Py-H$^+$) moiety formed in course of α-H$^+$ abstraction must be stable in the presence of MAO at least for a short time. In contrast to Al^{i}Bu$_3$ and most probably because of its size, MAO neither effectively blocks the pyridine moiety nor instantaneously deprotonates the Py-H$^+$ moiety, which explains both for the ROMP propensity in the presence of MAO and the ROMP-inactivity in the presence of Al^{i}Bu$_3$. In fact, as outlined earlier,[8] higher MAO concentrations result in larger fractions of ROMP-derived units in E-NBE copolymers. Any additional α-H$^+$ elimination in course of the copolymerization would regenerate the ROMP-active species, however, in view of the high propensity of the system to undergo cross metathesis with E (*vide supra*), only very few additional ROMP-derived poly(NBE) sequences can be expected to form (presumably <1% with respect to the initial amount of pre-catalyst). Instead, because of the instability of the Zr-methylidenes at elevated temperature, polymerization quickly comes to an end, which is indeed observed. What would be needed to boost productivity is an internal olefin that forms a more stable alkylidene in course of the cross metathesis with the Zr-alkylidene. Unfortunately, internal olefins are unable to undergo VIP.

Conclusions

Three new complexes, **L′Zr(CH$_3$)$_2$**, **L′Zr(Bn)$_2$** and **L′Zr(CH$_2$SiMe$_3$)$_2$**, based on modifications of **L′ZrCl$_2$** have been synthesized. These compounds are thermally stable and do not allow for the generation of alkylidenes, neither *via* thermolysis nor *via* the addition of phosphines. The corresponding cations were prepared *in situ* upon activation with $[Ph_3C]^+[B(C_6F_5)_4]^-$. The aluminum-free monoalkyl cations are able to produce predominantly *cis*, ROMP-derived poly(NBE) instead of VIP-derived poly(NBE) in NBE homopolymerization. The formation of alkylidenes in the absence of any aluminum reagent is proposed. Dialkyl complexes activated with $[Ph_3C]^+[B(C_6F_5)_4]^-$ and Al^{i}Bu$_3$ exhibit moderate catalytic activity in E-NBE copolymerization, producing only VIP-type poly(NBE) and branched PE with vinyl terminals. Polymer structures are considered to be a result of the high propensity of Al^{i}Bu$_3$ to react with the pyridyl-

moiety in $[\mathbf{L'ZrR}]^+$ (R = CH_3, Bn, CH_2SiMe_3). Similar to $\mathbf{L'ZrCl_2}$/MAO, which affords E-NBE copolymers containing both ROMP- and VIP-derived poly(NBE) in the PE chain with low productivity, $\mathbf{L'Zr(CH_2SiMe_3)_2}$/MAO allows for the synthesis of copolymers containing both (mostly *trans*) ROMP- and VIP-derived NBE sequences within the same polymer chain, *i.e.* poly(NBE)$_{ROMP}$-*co*-poly(NBE)$_{VIP}$-*co*-poly(E), through an α-H^+ elimination/addition process. By contrast, $\mathbf{L'Zr(CH_3)_2}$/MAO and $\mathbf{L'Zr(Bn)_2}$/MAO produce poly(NBE)$_{VIP}$-*co*-poly(E) without any ROMP-derived poly(NBE) sequences. We attribute the incapability of $\mathbf{L'Zr(CH_3)_2}$/MAO and $\mathbf{L'Zr(Bn)_2}$/MAO to promote the ROMP of NBE to the low stability of $\mathbf{L'Zr{=}CHR}$ (R = H, Ph) and their high propensity to undergo cross-metathesis with E. Finally, implications on the copolymerization of α-olefins (E) with NBE using "standard" metallocenes are clear. Apart from high NBE concentrations (catalyst : NBE > 1 : 5000), copolymerizations must be MAO-*co*-catalyzed and the catalyst, which ever, must allow for α-H^+ elimination in order to observe ROMP-derived structures. This is in most copolymerization systems not the case. In fact, particularly industrial large-volume systems sometimes contain substantial amounts of aluminum alkyls, which not only promote chain transfer and increase productivity[70–72] but also effectively prevent the formation of any ROMP-active sites by blocking any Lewis-basic groups.

Experimental

All manipulations were carried out using standard Schlenk or dry box techniques under an argon or nitrogen atmosphere unless specified otherwise. Deuterated solvents for NMR measurements were degassed by several freeze–pump–thaw cycles and stored inside a glove box. Benzene-d_6 and toluene-d_8 were dried and distilled from sodium/benzophenone; CD_2Cl_2 was distilled from P_2O_5; $C_2D_2Cl_4$ and *o*-$C_6D_4Cl_2$ were distilled from CaH_2. THF, diethyl ether, toluene, *n*-pentane and CH_2Cl_2 were deoxygenated by sparging with N_2 and passed through a triple-column solvent purification system (MBraun, Garching, Germany). Commercially available reagents for synthesis, *i.e.* methylmagnesium bromide solution (3.0 M in diethyl ether), benzylmagnesium chloride solution (1.0 M in diethyl ether), (trimethylsilyl)methylmagnesium chloride solution (1.0 M in diethyl ether), triisobutylaluminum solution (1.1 M in toluene) and $[Ph_3C]^+[B(C_6F_5)_4]^-$ were used without further purification. Methylalumoxane (MAO, 10 wt% solution in toluene) was purchased from Sigma-Aldrich, Germany. The toluene was removed *in vacuo* and the remaining white powder was dried *in vacuo* at 80 °C overnight to remove any free $AlMe_3$. Celite was dried *in vacuo* at 180 °C for two days prior to use. Before charging the autoclave, ethylene (E) gas was purified by passing it through columns filled with Cu-catalyst (BASF R3-11G) and 3 Å molecular sieves. All homopolymerization reactions of NBE were performed in Schlenk tubes under N_2 atmosphere. The homopolymerization of E and all copolymerizations of E with NBE were carried out in a Büchi-Uster pressure reactor equipped with a Huber thermostat. The ethylene pressure was kept constant and E-consumption was monitored with the aid of a Büchi pressflow bpc 6010 flow controller.

^{1}H and ^{13}C NMR spectra were recorded at 400 and 100 MHz, respectively, on a Bruker Avance III 400 spectrometer at 25 °C unless noted otherwise. Chemical shifts are reported in ppm and referenced to tetramethylsilane (TMS). All ^{1}H and ^{13}C NMR data of the ethylene homo- and E-NBE copolymers were measured at 100 °C except where noted. Molecular weights and molecular weight distributions were obtained by high-temperature gel permeation chromatography (HT-GPC) on an Agilent PL-GPC 220 system equipped with three consecutive PL gel 5 μm MIXED-C 300 × 7.5 mm columns with 1,2,4-trichlorobenzene as the solvent at 160 °C. The flow rate was set to 1 mL min^{-1}. The GPC system was calibrated with narrow polystyrene (PS) standards purchased from Polymer Labs with the molecular weights in the range of 162–6 035 000 g mol^{-1} (Easi Vial-red, yellow and green, Fig. S23†). Melting points and glass transition temperature were measured by differential scanning calorimetry (DSC) under N_2 atmosphere on a Perkin-Elmer DSC 4000 at a heat rate of 10 °C min^{-1}.

$\mathbf{L'Zr(CH_3)_2}$

To a solution of $\mathbf{L'ZrCl_2}$ (300 mg, 0.396 mmol) in diethyl ether (20 mL) at −35 °C was added MeMgBr (3.0 M in diethyl ether, 0.30 mL, 0.911 mmol). The solution became a suspension within 10 min and was stirred overnight at room temperature in the dark. After the removal of the solvent, the yellow residue was dissolved in toluene (10 mL) and the insoluble solid was filtered off through a pad of celite. The solvent was removed *in vacuo* to give a brown solid. Yield: 270 mg (80.5%). The solid was recrystallized from diethyl ether at −35 °C to give light-yellow crystals. ^{1}H NMR (C_6D_6): δ = 8.56 (dd, J = 7.7, 0.7 Hz, 1H), 7.62 (dd, J = 7.6, 1.0 Hz, 1H), 7.40 (td, J = 7.5, 1.4 Hz, 1H), 7.12 (td, J = 7.5, 1.2 Hz, 1H), 6.80 (dd, J = 7.9, 7.5 Hz, 1H), 6.72 (dd, J = 7.4, 1.0 Hz, 1H), 6.65 (s, 4H), 5.46 (dd, J = 8.0, 1.0 Hz, 1H), 2.14 (d, J = 10.9 Hz, 18H), 2.02 (d, J = 8.9 Hz, 12H), 0.46–0.41 (m, 6H), 0.12 (s, 6H, Zr–CH_3). ^{1}H NMR (CD_2Cl_2): δ = 8.09 (d, J = 7.7 Hz, 1H), 7.50 (td, J = 7.4, 1.7 Hz, 1H), 7.43–7.33 (m, 2H), 7.08 (d, J = 7.5 Hz, 1H), 6.62 (s, 4H), 6.53 (d, J = 7.3 Hz, 1H), 5.64 (d, J = 8.1 Hz, 1H), 2.18 (s, 6H), 2.04 (s, 6H), 1.96 (d, J = 11.7 Hz, 18H), 0.51–0.41 (m, 6H), −0.38 (s, 6H, Zr–CH_3). ^{13}C NMR (C_6D_6): δ = 164.8, 157.9, 148.8, 145.0, 143.4, 141.1, 139.1, 138.8, 136.2, 130.8, 130.2, 128.9, 128.7, 127.1, 123.8, 117.4, 109.0, 97.3, 41.4 (Zr–CH_3), 24.2, 21.3, 14.0, 11.5, 3.3. Elemental analysis calcd (%) for $C_{42}H_{53}BN_2SiZr(CH_2Cl_2)_{0.5}$: C 67.30, H 7.18, N 3.69; found: C 67.35, H 7.45, N 3.62.

$\mathbf{L'Zr(Bn)_2}$

To a solution of $\mathbf{L'ZrCl_2}$ (100 mg, 0.132 mmol) in diethyl ether (8 mL) at −35 °C was added benzylMgCl (1.0 M in diethyl ether, 0.29 mL, 0.29 mmol). The solution became a suspension within 5 min and was stirred overnight at room temperature in the dark. After the removal of the insoluble solid through celite, the solution was concentrated to ~1 mL and cooled to −35 °C overnight to afford a yellow solid. Yield:

68 mg (48.7%). The solid was recrystallized from diethyl ether at −35 °C to give yellow crystals. ^{1}H NMR (CD_2Cl_2): δ = 7.50 (dd, J = 7.6, 0.7 Hz, 1H), 7.45–7.33 (m, 2H), 7.29 (td, J = 7.4, 1.2 Hz, 1H), 7.21 (dd, J = 8.0, 7.4 Hz, 1H), 6.98 (t, J = 7.7 Hz, 4H), 6.77 (t, J = 7.3 Hz, 2H), 6.69–6.59 (m, 9H), 5.77 (dd, J = 8.1, 0.8 Hz, 1H), 2.20 (s, 6H), 2.06, 1.93 (d, J = 52 Hz, 2H, Zr–CH_2Ph), 2.03, 1.90 (d, J = 52 Hz, 2H, Zr–CH_2Ph), 1.95 (s, 12H), 1.86 (s, 6H), 1.76 (s, 6H), 0.49 (s, 6H). ^{13}C NMR (CD_2Cl_2): δ = 164.7, 158.8, 148.3, 147.4, 145.7, 143.3, 141.02, 138.9, 138.1, 136.0, 130.7, 130.4, 129.2, 128.6, 128.4, 128.2, 127.0, 125.4, 121.6, 118.3, 108.9, 99.0, 68.3 (Zr–CH$_2$Ph), 23.9, 21.3, 13.8, 11.3, 2.7. Elemental analysis calcd (%) for $C_{54}H_{61}BN_2SiZr(CH_2Cl_2)_{0.5}$: C 71.88, H 6.86, N 3.08; found: C 71.98, H 7.08, N 3.13.

L′Zr(CH$_2$SiMe$_3$)$_2$

To a solution of **L′ZrCl$_2$** (100 mg, 0.132 mmol) in diethyl ether (8 mL) at −35 °C was added Me_3SiCH_2MgCl (1.0 M in diethyl ether, 0.29 mL, 0.29 mmol). The solution became a suspension within 10 min and was stirred overnight at room temperature in the dark. After the removal of the insoluble solid through celite, the solution was concentrated to ∼0.5 mL and cooled to −35 °C overnight to give yellow crystals. Yield: 76 mg (61.3%). ^{1}H NMR (CD_2Cl_2): δ = 8.07 (d, J = 7.4 Hz, 1H), 7.56 (td, J = 7.4, 1.5 Hz, 1H), 7.42 (dd, J = 7.5, 1.4 Hz, 1H), 7.36 (td, J = 7.4, 1.0 Hz, 1H), 7.07 (t, J = 7.7 Hz, 1H), 6.62 (s, 4H), 6.56 (d, J = 7.3 Hz, 1H), 5.68 (d, J = 8.0 Hz, 1H), 2.19 (d, J = 2.7 Hz, 12H), 2.10 (s, 6H), 1.97 (s, 12H), 0.58, 0.10 (d, J = 192 Hz, 2H, Zr–CH_2SiMe$_3$), 0.54 (m, 6H), 0.56, 0.07 (d, J = 196 Hz, 2H, Zr–CH_2SiMe$_3$), −0.20 (s, 18H). ^{13}C NMR (CD_2Cl_2): δ = 164.2, 158.1, 147.6, 146.9, 143.3, 141.0, 138.8, 137.4, 136.4, 131.7, 130.1, 128.5, 128.4, 128.2, 124.8, 118.4, 108.6, 98.7, 58.2 (Zr–CH$_2$SiMe$_3$), 24.0, 21.3, 15.5, 14.9, 12.6, 3.6, 2.9. Elemental analysis calcd (%) for $C_{48}H_{69}BN_2Si_3Zr(Et_2O)$: C 66.83, H 8.52, N 3.00; found: C 66.36, H 8.49, N 3.26.

In situ preparation of [L′Zr(CH$_3$)]$^+$[B(C$_6$F$_5$)$_4$]$^-$

To a solution of **L′Zr(CH$_3$)$_2$** (10.0 mg, 11.8 μmol) in CD_2Cl_2 (0.3 mL) was added a solution of $[Ph_3C]^+[B(C_6F_5)_4]^-$ (10.9 mg, 11.8 μmol) in CD_2Cl_2 (0.3 mL) at room temperature. ^{1}H and ^{13}C NMR spectra were measured immediately and were indicative for the complete formation of **[L′Zr(CH$_3$)]$^+$[B(C$_6$F$_5$)$_4$]$^-$**. ^{1}H NMR (CD_2Cl_2): δ = 7.87 (dd, J = 8.2, 7.7 Hz, 1H), 7.84–7.77 (m, 2H), 7.57 (d, J = 6.6 Hz, 1H), 7.35 (s, 1H), 7.31–7.24 (m, 8H), 7.24–7.18 (m, 3H), 7.11 (ddd, J = 2.9, 2.2, 1.1 Hz, 6H), 6.95 (d, J = 1.8 Hz, 1H), 6.70 (d, J = 1.4 Hz, 1H), 6.56 (dd, J = 8.3, 1.0 Hz, 1H), 6.45 (s, 1H), 2.45–2.37 (m, 9H), 2.27 (s, 3H), 2.24 (s, 3H), 2.18 (s, 3H, Ph$_3$C–CH_3), 2.09 (d, J = 4.6 Hz, 6H), 1.92 (s, 3H), 1.74 (s, 3H), 1.49 (s, 3H), 0.95 (s, 3H), 0.56 (s, 3H), −0.05 (s, 3H, Zr–CH_3). ^{13}C NMR (CD_2Cl_2): δ = 164.2, 160.2, 150.2, 150.2, 149.5, 144.2, 142.3, 139.6, 138.3, 137.9, 136.5, 135.5, 135.1, 132.5, 131.4, 131.0, 130.8, 130.3, 129.6, 129.1, 128.5, 128.2, 127.5, 126.7, 126.3, 123.7, 115.2, 111.3, 104.6, 52.9 (Zr–CH$_3$), 37.9, 30.6, 28.4, 26.3, 25.9, 22.6, 20.5, 17.0, 15.8, 12.8, 11.7, 7.1, 3.8. ^{19}F NMR (CD_2Cl_2): δ = −133.0 (d, J = 13.0 Hz), −163.7 (t, J = 21.1 Hz), −165.1 to −170.3 (m).

[L′Zr(CH$_3$)Et$_2$O]$^+$[B(C$_6$F$_5$)$_4$]$^-$

A solution of $[Ph_3C]^+[B(C_6F_5)_4]^-$ (54.5 mg, 59.0 μmol) in CH_2Cl_2 (1.5 mL) was added to a solution of **L′Zr(CH$_3$)$_2$** (50.0 mg, 59.0 μmol) in CH_2Cl_2 (1.5 mL) at room temperature. The mixture was stirred for 10 min; then the solvent was removed *in vacuo*. The resulting residue was recrystallized from diethyl ether and *n*-pentane at room temperature to obtain a yellow solid. Yield: 65 mg (73.6%). ^{1}H NMR (CD_2Cl_2): δ = 7.91–7.85 (m, 1H), 7.85–7.77 (m, 2H), 7.57 (dd, J = 7.6, 0.9 Hz, 1H), 7.35 (s, 1H), 7.30–7.23 (m, 2H), 6.95 (d, J = 1.6 Hz, 1H), 6.70 (s, 1H), 6.56 (dd, J = 8.3, 0.9 Hz, 1H), 6.44 (s, 1H), 3.45 (q, J = 7.0 Hz, 4H), 2.46–2.36 (m, 9H), 2.26 (d, J = 11.2 Hz, 6H), 2.09 (d, J = 5.4 Hz, 6H), 1.92 (s, 3H), 1.74 (s, 3H), 1.49 (s, 3H), 1.16 (t, J = 7.0 Hz, 6H), 0.95 (s, 3H), 0.56 (s, 3H), −0.06 (s, 3H, Zr–CH_3). ^{13}C NMR (CD_2Cl_2): δ = 164.2, 160.2, 150.3, 150.2, 149.8, 144.2, 142.3, 139.6, 138.3, 137.9, 136.5, 135.5, 135.1, 132.5, 131.4, 131.0, 130.8, 130.3, 129.6, 128.5, 127.5, 126.7, 123.7, 115.2, 111.3, 104.6, 37.9, 28.4, 26.3, 25.9, 22.6, 20.5, 17.0, 15.8, 12.8, 11.7, 7.1, 3.8. The signal of Zr–CH$_3$ in the ^{13}C NMR spectrum was invisible due to an overlap with the signal of CD_2Cl_2. ^{19}F NMR (CD_2Cl_2): δ = −133.1 (d, J = 13.1 Hz), −163.7 (t, J = 20.9 Hz), −166.4 to −168.9 (m). Elemental analysis calcd (%) for $C_{69}H_{60}B_2F_{20}N_2OSiZr(CH_2Cl_2)_{0.5}$: C 55.78, H 4.11, N 1.87; found: C 55.60, H 4.20, N 1.96.

In situ preparation of [L′Zr(Bn)]$^+$[B(C$_6$F$_5$)$_4$]$^-$

To a solution of **L′Zr(Bn)$_2$** (13.0 mg, 12.3 μmol) in CD_2Cl_2 (0.3 mL) was added a solution of $[Ph_3C]^+[B(C_6F_5)_4]^-$ (11.3 mg, 12.3 μmol) in CD_2Cl_2 (0.3 mL) at room temperature. ^{1}H and ^{13}C NMR spectra were measured immediately and were indicative for the complete conversion of **[L′Zr(Bn)]$^+$[B(C$_6$F$_5$)$_4$]$^-$**. ^{1}H NMR (CD_2Cl_2): δ = 8.01 (t, J = 7.9 Hz, 1H), 7.80–7.75 (m, 1H), 7.64 (dd, J = 13.9, 7.2 Hz, 2H), 7.29 (t, J = 7.3 Hz, 2H), 7.26–7.12 (m, 16H), 7.04 (t, J = 7.4 Hz, 1H), 6.94 (dt, J = 10.5, 7.8 Hz, 4H), 6.81 (dd, J = 16.3, 8.1 Hz, 3H), 6.63 (d, J = 7.9 Hz, 3H), 6.47–6.38 (m, 3H), 3.95 (s, 2H, Ph$_3$C–CH_2Ph), 2.41 (s, 3H), 2.40 (s, 3H), 2.38 (s, 3H), 2.37, 1.57 (d, J = 320 Hz, 1H, Zr–CH_2Ph), 2.34, 1.54 (d, J = 320 Hz, 1H, Zr–CH_2Ph), 2.29 (s, 3H), 2.24 (s, 3H), 2.22 (s, 3H), 2.07 (s, 3H), 1.93 (s, 3H), 1.51 (s, 3H), 1.08 (s, 3H), 0.81 (s, 3H), 0.68 (s, 3H). ^{13}C NMR (CD_2Cl_2): δ = 164.1, 160.6, 151.3, 149.2, 149.1, 147.2, 143.9, 142.9, 141.2, 141.0, 139.0, 136.5, 135.4, 135.1, 131.7, 131.5, 131.4, 130.7, 130.2, 130.1, 130.1, 129.8, 129.1, 128.7, 128.7, 128.0, 127.6, 126.7, 126.5, 126.3, 126.3, 126.3, 124.3, 123.9, 114.8, 111.8, 105.1, 64.0 (Zr–CH$_2$Ph), 59.0 (Ph$_3$$C$–CH$_2$Ph), 46.4 (Ph$_3$C–$CH_2$Ph), 28.0, 26.7, 23.5, 23.2, 20.6, 20.5, 16.7, 16.6, 13.4, 11.8, 7.0, 3.2. ^{19}F NMR (CD_2Cl_2): δ = −133.0 (d, J = 13.5 Hz), −163.7 (t, J = 21.1 Hz), −166.4 to −169.3 (m).

In situ preparation of [L′Zr(CH$_2$SiMe$_3$)]$^+$[B(C$_6$F$_5$)$_4$]$^-$ (partial conversion)

To a solution of **L′Zr(CH$_2$SiMe$_3$)$_2$** (4.7 mg, 5.0 μmol) in CD_2Cl_2 (0.3 mL) was added a solution of $[Ph_3C]^+[B(C_6F_5)_4]^-$ (4.6 mg, 5.0 μmol) in CD_2Cl_2 (0.3 mL) at room temperature and the mixture was stirred overnight. The ^{1}H NMR spectrum revealed

~28 mol% conversion of **L′Zr(CH$_2$SiMe$_3$)$_2$** to **[L′Zr(CH$_2$SiMe$_3$)]$^+$[B(C$_6$F$_5$)$_4$]$^-$** as evidenced by the ratio of intensities of (converted aromatic protons)/(converted + non-converted aromatic protons) (Fig. S40, ESI†).

General procedure for NBE homopolymerization

All preparations were carried out inside a glove box. Defined amounts of NBE were dissolved in toluene (40 mL) inside a Schlenk tube. Then a toluene solution (5 mL) of a defined amount of the pre-catalyst was added. The mixture was stirred for 5 min before the addition of a defined amount of $[Ph_3C]^+[B(C_6F_5)_4]^-$ in toluene (5 mL) and heated to the desired temperature. Polymerizations were quenched after 1 h by the addition of methanol (10 mL). The mixture was then poured into methanol (500 mL) containing concentrated HCl (10 mL). The polymer was collected by filtration and adequately washed with methanol and then dried *in vacuo* at 50 °C for 2 days.

General procedure for E homo- and E-NBE copolymerization

Samples were prepared inside a glove box. Polymerization reactions were conducted by using a Büchi glass reactor (500 mL), which was dried at 120 °C *in vacuo* for 2 h, cooled to 30 °C and purged with Ar gas before use. (a) $[Ph_3C]^+[B(C_6F_5)_4]^-$ and Al^{i}Bu$_3$-activation: a solution of NBE in toluene (*ca*. 240 mL), a solution of the pre-catalyst in toluene (5 mL) and a solution of a defined amount of Al^{i}Bu$_3$ in toluene were quickly introduced into the reactor and stirred (300 rpm) for 5 min at 30 °C before the addition of a solution of $[Ph_3C]^+[B(C_6F_5)_4]^-$ in toluene (5 mL). (b) MAO-activation: a solution of NBE in toluene (*ca*. 240 mL) and a solution of a defined amount of MAO in toluene (5 mL) were quickly introduced into the reactor and stirred (300 rpm) for 5 min at 30 °C before the addition of a solution of pre-catalysts in toluene (5 mL). The reactor was pressurized with ethylene gas once the mixture had reached the desired temperature. The polymerization reaction was quenched after 1 h by the addition of methanol (10 mL). The resulting mixture was then poured into methanol (500 mL) containing concentrated HCl (10 mL). The polymer was collected by filtration and washed with methanol. All the E-NBE copolymers were extracted extensively with THF at 50 °C overnight before filtration. The resulting polymers were adequately washed with methanol and then dried *in vacuo* at 50 °C for 2 days.

X-ray measurements and structure determination

Data were collected on a Bruker Kappa Apex 2 duo diffractometer at 100 K. Structures were solved using direct methods with refinement by full matrix least-squares of F^2, with the program system SHELXL 97 in connection with a multi-scan absorption correction.[73] All non-hydrogen atoms were refined anisotropically.

Acknowledgements

Financial support by the Deutsche Forschungsgemeinschaft (DFG, grant-nr: BU2174/14-1) is gratefully acknowledged.

References

1 A. L. McKnight and R. M. Waymouth, *Chem. Rev.*, 1998, **98**, 2587–2598.
2 G. J. P. Britovsek, V. C. Gibson and D. F. Wass, *Angew. Chem., Int. Ed.*, 1999, **38**, 428–447.
3 W. Kaminsky, *J. Chem. Soc., Dalton Trans.*, 1998, 1413–1418.
4 X. Li and Z. Hou, *Coord. Chem. Rev.*, 2008, **252**, 1842–1869.
5 J. Klosin, P. P. Fontaine and R. Figueroa, *Acc. Chem. Res.*, 2015, **48**, 2004–2016.
6 Y.-X. Chen and T. J. Marks, *Organometallics*, 1997, **16**, 3649–3657.
7 E. Y.-X. Chen and T. J. Marks, *Chem. Rev.*, 2000, **100**, 1391–1434.
8 M. R. Buchmeiser, S. Camadanli, D. Wang, Y. Zou, U. Decker, C. Kühnel and I. Reinhardt, *Angew. Chem.*, 2011, **123**, 3628–3633, (*Angew. Chem., Int. Ed.*, 2011, **50**, 3566–3571).
9 M. R. Buchmeiser, *Curr. Org. Chem.*, 2013, **17**, 2764–2775.
10 G. V. Narayana, G. Xu, D. Wang, W. Frey and M. R. Buchmeiser, *ChemPlusChem*, 2014, **79**, 151–162.
11 G. V. Narayana, G. Xu, D. Wang, M. Speiser, W. Frey and M. R. Buchmeiser, *Macromol. Chem. Phys.*, 2014, **215**, 2007–2013.
12 M. Wang, G. Xu, D. Wang, Y. Zou, W. Frey and M. R. Buchmeiser, *Polym. Chem.*, 2015, **6**, 3290–3304.
13 G. Xu, G. V. Narayana, M. Speiser, D. Wang, Y. Zou and M. R. Buchmeiser, *Macromol. Chem. Phys.*, 2014, **215**, 893–899.
14 Y. Zou, D. Wang, K. Wurst, C. Kühnel, I. Reinhardt, U. Decker, V. Gurram, S. Camadanli and M. R. Buchmeiser, *Chem. – Eur. J.*, 2011, **17**, 13832–13846.
15 M. Bochmann, *J. Chem. Soc., Dalton Trans.*, 1996, 255–270.
16 R. Collins, A. Russell and P. Mountford, *Appl. Petrochem. Res.*, 2015, 1–19.
17 M. Bochmann, *J. Organomet. Chem.*, 2004, **689**, 3982–3998.
18 L. Resconi, R. L. Jones, A. L. Rheingold and G. P. A. Yap, *Organometallics*, 1996, **15**, 998–1005.
19 J. Pinkas, I. Cisarova, J. Kubista, M. Horacek and M. Lamac, *Dalton Trans.*, 2013, **42**, 7101–7110.
20 W.-Y. Lee and L.-C. Liang, *Inorg. Chem.*, 2008, **47**, 3298–3306.
21 K. C. Jantunen, B. L. Scott and J. L. Kiplinger, *J. Alloys Compd.*, 2007, **444–445**, 363–368.
22 P. D. Bolton, N. Adams, E. Clot, A. R. Cowley, P. J. Wilson, M. Schröder and P. Mountford, *Organometallics*, 2006, **25**, 5549–5565.
23 L.-C. Liang, P.-S. Chien, Y.-C. Hsiao, C.-W. Li and C.-H. Chang, *J. Organomet. Chem.*, 2011, **696**, 3961–3965.
24 S. Gentil, N. Pirio, P. Meunier, J. C. Gallucci, J. D. Schloss and L. A. Paquette, *Organometallics*, 2000, **19**, 4169–4172.
25 M. Bochmann, S. J. Lancaster, M. B. Hursthouse and K. M. A. Malik, *Organometallics*, 1994, **13**, 2235–2243.
26 M. Bochmann and S. J. Lancaster, *Organometallics*, 1993, **12**, 633–640.
27 J. Sassmannshausen, A. Track and F. Stelzer, *Organometallics*, 2006, **25**, 4427–4432.

28 S. R. Golisz and J. E. Bercaw, *Macromolecules*, 2009, **42**, 8751–8762.
29 R. C. Klet, C. N. Theriault, J. Klosin, J. A. Labinger and J. E. Bercaw, *Macromolecules*, 2014, **47**, 3317–3324.
30 E. Despagnet-Ayoub, L. M. Henling, J. A. Labinger and J. E. Bercaw, *Dalton Trans.*, 2013, **42**, 15544–15547.
31 Y.-X. Chen, P.-F. Fu, C. L. Stern and T. J. Marks, *Organometallics*, 1997, **16**, 5958–5963.
32 C. P. Casey and D. W. Carpenetti Ii, *J. Organomet. Chem.*, 2002, **642**, 120–130.
33 N. A. Petasis and D. K. Fu, *J. Am. Chem. Soc.*, 1993, **115**, 7208–7214.
34 B. J. J. v. de Heisteeg, G. Schat, O. S. Akkerman and F. Bickelhaupt, *Tetrahedron Lett.*, 1987, **28**, 6493–6496.
35 J. A. v. Doorn, H. v. d. Heijden and A. G. Orpen, *Organometallics*, 1995, **14**, 1278–1283.
36 L. R. Gilliom and R. H. Grubbs, *Organometallics*, 1986, **5**, 721–724.
37 J. D. Meinhart, E. V. Anslyn and R. H. Grubbs, *Organometallics*, 1989, **8**, 583–589.
38 H. van der Heijden and B. Hessen, *J. Chem. Soc., Chem. Commun.*, 1995, 145–146.
39 W. Weng, L. Yang, B. M. Foxman and O. V. Ozerov, *Organometallics*, 2004, **23**, 4700–4705.
40 I. Furuta, S.-I. Kimura and M. Iwama, Physical Constants of Rubbery Polymers, in *Polymer Handbook*, ed. E. A. Grulke, 1999, vol. 1.
41 B. C. Bailey, F. Basuli, J. C. Huffman and D. J. Mindiola, *Organometallics*, 2006, **25**, 3963–3968.
42 B. C. Bailey, H. Fan, J. C. Huffman, M.-H. Baik and D. J. Mindiola, *J. Am. Chem. Soc.*, 2007, **129**, 8781–8793.
43 B. C. Bailey, J. C. Huffman, D. J. Mindiola, W. Weng and O. V. Ozerov, *Organometallics*, 2005, **24**, 1390–1393.
44 C. M. Brammell, E. J. Pelton, C.-H. Chen, A. A. Yakovenko, W. Weng, B. M. Foxman and O. V. Ozerov, *J. Organomet. Chem.*, 2011, **696**, 4132–4137.
45 A. R. Fout, J. Scott, D. L. Miller, B. C. Bailey, M. Pink and D. J. Mindiola, *Organometallics*, 2009, **28**, 331–347.
46 M. D. Fryzuk, P. B. Duval, B. O. Patrick and S. J. Rettig, *Organometallics*, 2001, **20**, 1608–1613.
47 L. R. Gilliom and R. H. Grubbs, *J. Am. Chem. Soc.*, 1986, **108**, 733–742.
48 M. Kamitani, B. Pinter, C.-H. Chen, M. Pink and D. J. Mindiola, *Angew. Chem., Int. Ed.*, 2014, **53**, 10913–10915.
49 R. F. Jordan, C. S. Bajgur, R. Willett and B. Scott, *J. Am. Chem. Soc.*, 1986, **108**, 7410–7411.
50 X. Yang, C. L. Stern and T. J. Marks, *J. Am. Chem. Soc.*, 1991, **113**, 3623–3625.
51 M. Bochmann and M. J. Sarsfield, *Organometallics*, 1998, **17**, 5908–5912.
52 K. Liu, Q. Wu, W. Gao and Y. Mu, *Dalton Trans.*, 2011, **40**, 4715–4721.
53 K. Liu, Q. Wu, X. Luo, W. Gao and Y. Mu, *Dalton Trans.*, 2012, **41**, 3461–3467.
54 Y. Luo, X. Feng, Y. Wang, S. Fan, J. Chen, Y. Lei and H. Liang, *Organometallics*, 2011, **30**, 3270–3274.
55 N. Naga and K. Mizunuma, *Polymer*, 1998, **39**, 5059–5067.
56 B. Wang, T. Tang, Y. Li and D. Cui, *Dalton Trans.*, 2009, 8963–8969.
57 X.-Y. Wang, Y.-X. Wang, Y.-S. Li and L. Pan, *Macromolecules*, 2015, **48**, 1991–1998.
58 T. Xiao, J. Wang, Y. Zhang, W. Gao and Y. Mu, *J. Organomet. Chem.*, 2008, **693**, 1195–1202.
59 X. Li, X. Wang, X. Tong, H. Zhang, Y. Chen, Y. Liu, H. Liu, X. Wang, M. Nishiura, H. He, Z. Lin, S. Zhang and Z. Hou, *Organometallics*, 2013, **32**, 1445–1458.
60 M. Nabika, H. Katayama, T. Watanabe, H. Kawamura-Kuribayashi, K. Yanagi and A. Imai, *Organometallics*, 2009, **28**, 3785–3792.
61 P. Sudhakar, *J. Polym. Sci., Part A: Polym. Chem.*, 2008, **46**, 444–452.
62 I. Tritto, L. Boggioni, C. Zampa and D. R. Ferro, *Macromolecules*, 2005, **38**, 9910–9919.
63 S. M. Baldwin, J. E. Bercaw, L. M. Henling, M. W. Day and H. H. Brintzinger, *J. Am. Chem. Soc.*, 2011, **133**, 1805–1813.
64 P. D. Bolton, E. Clot, A. R. Cowley and P. Mountford, *Chem. Commun.*, 2005, 3313–3315.
65 P. D. Bolton, E. Clot, A. R. Cowley and P. Mountford, *J. Am. Chem. Soc.*, 2006, **128**, 15005–15018.
66 G. Theurkauff, A. Bondon, V. Dorcet, J.-F. Carpentier and E. Kirillov, *Angew. Chem., Int. Ed.*, 2015, **54**, 6343–6346.
67 S. Hermanek, *Chem. Rev.*, 1992, **92**, 325–362.
68 F. Teixidor, M. A. Flores, C. Viñas, R. Sillanpää and R. Kivekäs, *J. Am. Chem. Soc.*, 2000, **122**, 1963–1973.
69 Y.-L. Rao, H. Amarne, S.-B. Zhao, T. M. McCormick, S. Martić, Y. Sun, R.-Y. Wang and S. Wang, *J. Am. Chem. Soc.*, 2008, **130**, 12898–12900.
70 T. Shiono, S. Yoshida, H. Hagihara and T. Ikeda, *Appl. Catal., A*, 2000, **200**, 145–152.
71 S. S. Reddy, G. Shashidhar and S. Sivaram, *Macromolecules*, 1993, **26**, 1180–1182.
72 H. Hammawa, T. M. Mannan, D. T. Lynch and S. E. Wanke, *J. Appl. Polym. Sci.*, 2004, **92**, 3549–3560.
73 G. M. Sheldrick, *Program package SHELXTL V.5.1*, Bruker Analytical X-Ray Instruments Inc, Madison, USA, 1997.

